

# Characterizing *Kepler* Asteroseismic Targets<sup>\*</sup>

J. Molenda-Żakowicz<sup>1</sup>†, D. W. Latham<sup>2</sup>, G. Catanzaro<sup>3</sup>, A. Frasca<sup>3</sup>, and S. N. Quinn<sup>2</sup>

<sup>1</sup> *Astronomical Institute of the University of Wrocław, ul. Kopernika 11, 51-622 Wrocław, Poland*

<sup>2</sup> *Harvard-Smithsonian Center for Astrophysics, 60 Garden Street, Cambridge, MA 02138, USA*

<sup>3</sup> *INAF - Osservatorio Astrofisico di Catania, Via S. Sofia 78, 95123 Catania, Italy*

Accepted 2010 November 3. Received 2010 November 3; in original form 2010 July 13

## ABSTRACT

Stellar structure and evolution can be studied in great detail by asteroseismic methods, provided data of high precision are available. We determine the effective temperature ( $T_{\text{eff}}$ ), surface gravity ( $\log g$ ), metallicity, and the projected rotational velocity ( $v \sin i$ ) of 44 *Kepler* asteroseismic targets using our high-resolution ( $R > 20,000$ ) spectroscopic observations; these parameters will then be used to compute asteroseismic models of these stars and to interpret the *Kepler* light curves. We use the method of cross correlation to measure the radial velocity ( $RV$ ) of our targets, while atmospheric parameters are derived using the ROTFIT code and spectral synthesis method. We discover three double-lined spectroscopic binaries, HIP 94924, HIP 95115, and HIP 97321 – for the last system, we provide the orbital solution, and we report two suspected single-lined spectroscopic binaries, HIP 94112 and HIP 96062. For all stars from our sample we derive  $RV$ ,  $v \sin i$ ,  $T_{\text{eff}}$ ,  $\log g$ , and metallicity, and for six stars, we perform a detailed abundance analysis. A spectral classification is done for 33 targets. Finally, we show that the early-type star HIP 94472 is rotating slowly ( $v \sin i = 13 \text{ km s}^{-1}$ ) and we confirm its classification to the Am spectral type which makes it an interesting and promising target for asteroseismic modeling. The comparison of the results reported in this paper with the information in the *Kepler* Input Catalog (KIC) shows an urgent need for verification and refinement of the atmospheric parameters listed in the KIC. That refinement is crucial for making a full use of the data delivered by *Kepler* and can be achieved only by a detailed ground-based study.

**Key words:** space vehicles: *Kepler* – stars: abundances – stars: fundamental parameters – stars: binaries: spectroscopic.

## 1 INTRODUCTION

The NASA space mission *Kepler*<sup>1</sup> was successfully launched in March 2009 with the goal of detecting Earth-size and larger planets by means of the method of photometric transits (Borucki et al. 2009). Having been in orbit since one year, *Kepler* has already discovered seven giant planets and delivered photometric data for hundreds of stars selected as asteroseismic targets by the *Kepler* Asteroseismic Science Consortium, KASC<sup>2</sup> (Christensen-Dalsgaard et al. 1997).

The aim of the investigation carried out by KASC is

a study the internal structure of the stars by means of asteroseismic methods (see Gilliland et al. 2010; Chaplin et al. 2010). In particular, the asteroseismic analysis of stars showing solar-like oscillations allows to derive the stars' mean density which, when combined with models, yields the stellar mass and radius. The last parameter is one of the key characteristics needed to infer the diameters of transiting objects and as such is crucial for the study of the planetary systems discovered by *Kepler*.

The asteroseismic analysis, though, is not the only method which can yield precise values of the radius of the planet-hosting star and thereby the diameter of the planet. As described in detail by Sozzetti et al. (2007), the stellar density is one of the primary quantities constrained by the analysis of the light curve of a transiting body. Therefore, these two independent ways of deriving the stellar density can be used as a test of the physics involved in the computations. Moreover, as shown by Christensen-Dalsgaard et al. (2010), the density derived from the analysis of the light

<sup>\*</sup> The data used in this paper have been obtained at the Catania Astrophysical Observatory (Italy) the F.L. Whipple Observatory, Arizona (USA), and the Oak Ridge Observatory, Massachusetts (USA).

† E-mail: molenda@astro.uni.wroc.pl

<sup>1</sup> <http://kepler.nasa.gov/>

<sup>2</sup> <http://astro.phys.au.dk/KASC>

curve can be used to select the correct value of the large separation ( $\Delta\nu$ ) of the frequencies of solar-like oscillators for which the low signal-to-noise of the data does not allow to detect individual frequencies and makes the asteroseismic analysis inconclusive.

Since the asteroseismic modeling requires accurate values of the effective temperature ( $T_{\text{eff}}$ ), the metallicity and the surface gravity ( $\log g$ ) or an equivalent parameter describing the luminosity of the star, one of the purposes of the KASC is deriving these values from coordinated ground-based spectroscopic and photometric observations as described by Uytterhoeven et al. (2010) and Molenda-Żakowicz et al. (2010). These efforts are needed because the stated precision of the atmospheric parameters provided in the Kepler Input Catalog (KIC)<sup>3</sup> and derived from the photometric observations acquired in the Sloan filters (Latham et al. 2005), is 200 K in  $T_{\text{eff}}$ , and 0.5 dex in  $\log g$  and [Fe/H] which is too low for an asteroseismic modeling. Moreover, a significant fraction of *Kepler* asteroseismic targets are missing the information on  $T_{\text{eff}}$ ,  $\log g$  and [Fe/H] in the KIC.

This paper is a sequel of a series started in 2006 (see Catanzaro et al. 2010, and the references therein) which aims at deriving atmospheric parameters of stars selected as *Kepler* asteroseismic targets by J.M.-Ż and A.F. in the first run of the *Kepler* proposals. In this paper, we provide  $T_{\text{eff}}$ ,  $\log g$ , the metal abundance, as well as the projected rotational velocity ( $v \sin i$ ) and the radial velocity ( $V_r$ ) for 44 stars. The information derived by us will be used by the KASC to construct the evolutionary and asteroseismic models of these stars and to determine their radii as described by Stello et al. (2009). The information on  $v \sin i$  will help select candidates for the long-term monitoring of *Kepler* asteroseismic targets while the measurements of  $RV$  will allow to detect new single- and double-lined spectroscopic binaries in the *Kepler* field. The latter systems are particularly important for the study of the planetary systems since for stars with the orbital solutions the mass of the star can be computed which allows to determine the mass of the transiting planet.

## 2 OBSERVATIONS AND DATA REDUCTION

The observations were performed at the *INAF-Osservatorio Astrofisico di Catania* (OAC), Mt. Etna, Italy (63 spectrograms), the Oak Ridge Observatory (ORO), Harvard, Massachusetts (162 spectrograms), and the F.L. Whipple Observatory (FLWO), Mount Hopkins, Arizona (95 spectrograms). We made use also of the archival spectroscopic observations acquired at the Multiple Mirror Telescope (MMT), Mount Hopkins, Arizona (10 spectrograms) before it was converted to the monolithic 6.5-m mirror. We acquired a total of 288 spectrograms; 6 of our targets were observed more than 20 times, 19 stars, 2-3 times, while for the remaining 19 targets we acquired single spectrograms.

At OAC, we used the 91-cm telescope and FRESKO, a fiber-fed REOSC echelle spectrograph, that allows to obtain  $R=21\,000$  spectra in the range of 4300–6800 Å in 19 orders.

The gaps between the first six orders decrease from 27 to 4 Å going from the red part of the spectrum to the blue. Then, the spectral ranges covered by the consecutive orders starts to overlap. The spectra were recorded on a thinned, back-illuminated (SITE) CCD with 1024 x 1024 pixels of 24 μm size, typical readout noise of 10 e<sup>-</sup> and gain of 2.5 e<sup>-</sup>/ADU. For the reduction of the spectrograms, we used the NOAO/IRAF package<sup>4</sup>. The reduction included the subtraction of the bias frame, trimming, correcting for the flat-field and the scattered light. The spectra were then extracted with the use of the `apall` task also provided by IRAF.

At ORO and FLWO, the spectra were acquired using 1.5-m telescopes and the CfA Digital Speedometers which are nearly identical instruments each with the resolving power  $R=35\,000$ . These echelle spectrographs, with photon-counting intensified Reticon detectors, record about 45 Å of spectrum in a single order centered at 5187 Å. The spectra were extracted and rectified by means of a special procedure developed for these observatories and described by Latham et al. (1992).

## 3 RADIAL VELOCITY

For stars observed at OAC, the radial velocity was derived with the cross-correlation method through the `fxcorr` task in IRAF. For stars of the spectral type F, G, and K we used Arcturus (K1.5 III,  $RV = -5.30 \text{ km s}^{-1}$  by Udry et al. (1999)) or 54 Aql (F8 V,  $RV = -0.20 \text{ km s}^{-1}$  by Evans (1967)) as the templates. For the early-type stars, we used HR 1389 (A2 V-IV,  $RV = 38.97 \text{ km s}^{-1}$  by Fekel (1999)).

The weighted mean radial velocities were calculated by averaging the measurements from all echelle orders, adopting the instrumental weight  $W_i = \sigma_i^2$  for each  $i$ -th order. The values of the  $\sigma_i^2$  errors were computed by the `fxcor` task in IRAF taking into account the height of the fitted peak and the antisymmetric noise (see Tonry & Davis, 1979). The uncertainties in the weighted means of  $RV$  were computed on the basis of  $\sigma_i^2$  in each echelle order as described, e.g., by Topping (1972).

For stars for which we acquired only two or three spectrograms, we computed both the external and the internal error of the weighted mean (see Topping 1972) and adopted the higher of the two as the representative uncertainty.

In order to estimate any possible systematic error of the  $RV$  derived from the spectrograms acquired at OAC, we performed a self-consistency check of the  $RV$  measured for Arcturus, one of our  $RV$  standards observed for 1.5 years covering the time-span of our observations. We derived  $RV$  of Arcturus using the first spectrum acquired for this star as the template. As a result, we found that the derived values are self-consistent with the rms precision of better than  $0.3 \text{ km s}^{-1}$ . An analogous analysis performed by Stefanik, Latham, & Torres (1999) shows that the  $RV$  derived from the CfA observations are accurate to better than  $0.2 \text{ km s}^{-1}$ .

The spectra acquired at CfA span a single echelle order centered on 5187 Å that includes the Mg b features.

<sup>3</sup> [http://archive.stsci.edu/kepler/kepler\\_fov/search.php](http://archive.stsci.edu/kepler/kepler_fov/search.php)

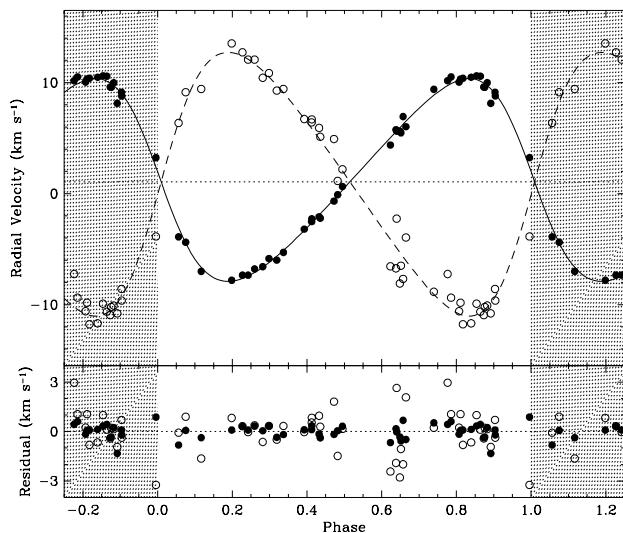
<sup>4</sup> IRAF is distributed by the National Optical Astronomy Observatory, which is operated by the Association of Universities for Research in Astronomy, Inc.

**Table 1.** The individual radial velocity measurements of 44 Kepler asteroseismic targets.

HIP	KIC-10	$\alpha_{2000}$	$\delta_{2000}$	Kep mag	HJD +2400000	$RV$ [km s <sup>-1</sup> ]	$\sigma$ [km s <sup>-1</sup> ]	Instrument	$T_{\text{exp}}$ [s]	S/N
91990	8343931	18:44:57.58	+44:21:32.3	8.25	54656.4941	9.75	0.83	FRESCO	3600	60
91990	8343931	18:44:57.58	+44:21:32.3	8.25	54667.3607	9.46	0.71	FRESCO	3600	95
92962	9139163	18:56:22.13	+45:30:25.3	8.33	54656.5414	-29.16	0.17	FRESCO	3600	70
92962	9139163	18:56:22.13	+45:30:25.3	8.33	54667.4454	-29.96	0.14	FRESCO	2700	80
97992	10162436	19:54:54.17	+47:08:43.0	8.61	54662.5474	-54.30	0.17	FRESCO	5400	60

**Table 3.** HIP 97321: Orbital Solution

$P = 1730.3 \pm 5.8$ d
$\gamma = 1.063 \pm 0.070$ km s <sup>-1</sup>
$K_A = 9.13 \pm 0.11$ km s <sup>-1</sup>
$K_B = 11.87 \pm 0.30$ km s <sup>-1</sup>
$e = 0.231 \pm 0.010$
$\omega_1 = 85.5^\circ \pm 2.9^\circ$
$T = \text{HJD } 2450219 \pm 14$
$a_A \sin i = 211.4 \pm 2.3 \times 10^6$ km
$a_B \sin i = 274.9 \pm 6.6 \times 10^6$ km
$M_A \sin^3 i = 0.865 \pm 0.046 M_\odot$
$M_B \sin^3 i = 0.666 \pm 0.024 M_\odot$
$q = 0.769 \pm 0.020$


**Figure 1.** *Top:* The  $RV$  light curve of the primary (dots) and the secondary (circles) component of the SB2 system HIP 97321. *Bottom:* The residuals of  $RV$  of the components left after subtracting the orbital motion.

To derive the stellar parameters and radial velocities, the observed spectra were cross-correlated against a library of synthetic spectra calculated by John Laird using Kurucz model atmospheres and a line list developed by Jon Morse. The details of the analysis are documented in Latham et al. (2002), along with a description of the procedures used to identify spectroscopic binaries and derive orbital solutions.

**The individual radial velocity measurements for**

**our program stars are given in Table 1. This Table is available only in the electronic form. Only a sample, containing the first four rows, and the last row, is presented.** In the first and the second column of this Table, we give the HIP number from the Hipparcos Catalogue (ESA 1997) and the KIC number from Kepler Input Catalog. Then, in the following columns, the right ascension and declination of the star for the epoch 2000, the Kepler magnitude of the star, the Heliocentric Julian Day of the middle of the exposure, the radial velocity and its standard error, and the name of the instrument used for acquiring the spectrum are quoted. In the two last columns, we list the exposure times and the signal-to-noise ratios for the spectrograms acquired with FRESCO; at the remaining observing sites, the exposure time was set to 1200 s, and the typical S/N was 15-20.

In Table 1, we do not list the errors of  $RV$  of the components of the double-lined spectroscopic binaries HIP 95575 and HIP 97321 for which the  $RV$  were computed using the TODCOR two-dimensional correlation technique (Zucker & Mazeh 1994) because TODCOR does not provide uncertainties for individual observations. Instead, in Fig. 1 we provide the rms velocity residuals from the orbital solution for the primary and secondary component of HIP 97321, which give a good overview of the velocity errors.

In Table 2, we list the HIP and KIC numbers of all the observed targets, their equatorial coordinates for the epoch 2000, the *Kepler* magnitude, the spectral type derived in this paper or adopted from the literature, the number of the acquired spectrograms, the time-span of the observations, the mean radial velocity and its standard deviation. Then, we list the sum of the residuals divided by the internal error estimate squared,  $\chi^2$ , and the probability that a star with constant velocity will have  $\chi^2$  values larger than the observed one,  $P(\chi^2)$ . For the spectroscopic binaries, in the last column we give the classification to the type of the spectroscopic variability. For 25 stars whose HIP numbers in Table 2 are typed bold face, the radial velocity given in this paper has been measured for the first time.

We note that the mean radial velocities given in Table 2 were calculated subtracting  $0.5 \text{ km s}^{-1}$  from each measurement of  $RV$  derived from the spectra acquired at OAC in order to put all the measurements on the native CfA system, as explained in Molenda-Żakowicz et al. (2007). To put these values on an absolute system,  $0.14 \text{ km s}^{-1}$  should be added to the CfA native velocities (see Stefanik, Latham, & Torres 1999, noting that the sign of the correction in that paper is in error.)

**Table 2.** The spectral type and the average radial velocity of the target stars.

HIP	KIC-10	$\alpha_{2000}$ ( <sup>h</sup> <sup>m</sup> <sup>s</sup> )	$\delta_{2000}$ ( <sup>°</sup> <sup>'</sup> <sup>''</sup> )	$Kp$ (mag)	SpT	$N$	Span (days)	$\langle RV \rangle$ (km s <sup>-1</sup> )	$\chi^2$	P( $\chi^2$ )
91990	8343931	18:44:57.58	+44:21:32.3	8.25	F5 V	2	11	9.08 ± 0.54	...	...
92962	9139163	18:56:22.13	+45:30:25.3	8.33	F8 V	2	11	-30.14 ± 0.39	...	...
<b>92983</b>	10454113	18:56:36.62	+47:39:23.1	8.62	F9 V	1	...	-24.14 ± 0.22	...	...
93108A	10124866	18:58:03.46	+47:11:29.9	7.58	G0 V	27	3606	-29.81 ± 0.12	59.4	0.00
93108B	10124866	18:58:03.46	+47:11:29.9	....	....	28	3606	-32.26 ± 0.15	87.9	0.00
93236	7944142	18:59:28.70	+43:43:59.4	7.82	K1 III	2	7	-1.00 ± 0.42	...	...
<b>93556</b>	11018874	19:03:19.20	+48:30:35.8	8.83	F6 V	2	17	0.65 ± 0.61	...	...
93594	4818496	19:03:39.26	+39:54:39.4	8.14	A1 V <sup>a</sup>	1	...	14.28 ± 7.82	...	...
93657	5774694	19:04:16.37	+41:00:11.4	8.31	G1 V	25	5479	-17.76 ± 0.13	40.1	0.01
<b>93703</b>	8547390	19:04:50.64	+44:41:28.9	8.38	K0 III	1	...	-41.66 ± 0.12	...	...
<b>93898</b>	8677933	19:07:12.19	+44:50:30.2	8.87	G0 IV	1	...	-14.41 ± 0.54	...	...
93951	11498538	19:07:46.85	+49:29:07.3	7.34	F4 V	1	...	-10.35 ± 0.43	...	...
<b>94071</b>	3733735	19:09:01.92	+38:53:59.6	8.37	F4 V	2	2874	3.10 ± 0.44	...	...
94112	3632418	19:09:26.83	+38:42:50.5	8.22	F8 V	1	...	-19.72 ± 0.15	...	SB1?
94239	12453925	19:11:00.70	+51:21:43.8	8.34	F5 V	1	...	4.15 ± 2.20	...	...
<b>94343</b>	6432054	19:12:09.53	+41:50:15.3	8.21	F0 <sup>b</sup>	1	...	19.58 ± 5.30	...	...
<b>94472</b>	12253106	19:13:38.78	+50:54:30.9	8.41	Am <sup>c</sup>	1	...	5.39 ± 1.39	...	...
94675	10068307	19:15:54.70	+47:03:40.5	8.18	F8 V	1	...	-15.22 ± 0.19	...	...
<b>94798</b>	11708170	19:17:18.50	+49:51:00.8	7.21	F1 V	2	3272	-9.72 ± 0.47	...	...
<b>94922</b>	11709006	19:18:56.54	+49:51:35.2	8.78	G1 V	3	2797	-0.09 ± 0.27	...	...
<b>94924</b>	4150611	19:18:58.20	+39:16:01.4	7.90	A5 V <sup>d</sup>	3	5	... <sup>h</sup>	...	SB2
94931	6278762	19:19:00.55	+41:38:04.6	8.72	K0 V <sup>e</sup>	23	9189	-121.52 ± 0.14	22.2	0.33
95115	3641446	19:20:59.16	+38:47:23.8	8.37	F1 V	1	...	... <sup>h</sup>	...	SB2
<b>95274</b>	10532461	19:23:01.94	+47:42:52.5	8.85	G8 V	3	2799	6.53 ± 0.21	...	...
<b>95438</b>	7820638	19:24:48.70	+43:31:18.5	7.95	G9 III	1	...	-19.53 ± 0.21	...	...
<b>95491</b>	10010623	19:25:25.82	+46:57:29.1	8.40	F4 V	2	4	-22.30 ± 0.30	...	...
<b>95548</b>	6862114	19:26:05.47	+42:19:34.1	8.01	A2 <sup>f</sup>	1	...	-11.11 ± 4.50	...	...
<b>95549</b>	3747220	19:26:05.93	+38:48:49.1	8.05	F1 V	1	...	-7.72 ± 1.05	...	...
95568	12258514	19:26:22.08	+50:59:14.1	8.08	G0	3	2799	-19.61 ± 0.15	...	...
95575	11506859	19:26:25.97	+49:27:55.0	7.90	K2.5 V <sup>g</sup>	3	5839	... <sup>h</sup>	...	SB2
<b>95580</b>	11189959	19:26:28.37	+48:52:14.9	8.21	A0 <sup>b</sup>	1	...	-8.14 ± 6.23	...	...
<b>95661</b>	11402951	19:27:32.81	+49:15:23.5	8.13	F0 V	1	...	-25.88 ± 3.39	...	...
95876	8561664	19:29:56.69	+44:41:22.9	7.78	F3 V	2	3308	4.97 ± 0.32	...	...
<b>96010</b>	3347643	19:31:16.22	+38:24:02.9	8.02	A2 <sup>b</sup>	2	5	-10.01 ± 3.71	...	...
96062	11031993	19:31:56.02	+48:35:34.2	8.47	F5 V	74	9481	-57.74 ± 0.17	70.3	SB1?
96528	5371516	19:37:27.70	+40:35:19.9	8.37	F6 IV	1	...	-5.56 ± 0.25	...	...
<b>96561</b>	7898839	19:37:51.72	+43:37:31.6	8.86	K0 V	2	2879	4.26 ± 0.32	...	...
<b>96775</b>	4574610	19:40:15.43	+39:40:58.4	8.83	F6 V	2	8	-44.53 ± 0.56	...	...
<b>97071</b>	11253226	19:43:39.62	+48:55:44.2	8.44	F5 IV	2	6	9.89 ± 0.17	...	...
<b>97236</b>	4484238	19:45:44.59	+39:30:13.2	8.56	F9 V	2	2771	-14.86 ± 0.65	...	...
<b>97316</b>	12317678	19:46:37.73	+51:01:13.5	8.74	F6 V	1	...	-26.39 ± 0.19	...	...
97321	8379927	19:46:41.30	+44:20:54.7	6.96	F8 V	44	5890	1.06 ± 0.07 <sup>i</sup>	...	SB2
<b>97341</b>	11255615	19:47:00.98	+48:55:55.2	8.81	F7 IV	2	4	-17.29 ± 0.13	...	...
97706	5557932	19:51:24.77	+40:44:07.4	8.14	G9 V	3	2760	-24.03 ± 1.39	...	...
<b>97992</b>	10162436	19:54:54.17	+47:08:43.0	8.61	F8 V	1	...	-54.80 ± 0.17	...	...

<sup>a</sup> Grenier et al. (1999), <sup>b</sup> Royal Observatory, Greenwich (1935), <sup>c</sup> Bidelman (1985), <sup>d</sup> Sato & Kuji (1990), <sup>e</sup> Wilson (1962), <sup>f</sup> Thompson et al. (1978), <sup>g</sup> Gray et al. (2003).<sup>h</sup> The individual radial velocities of the components are listed in Table 1.<sup>i</sup> The barycentric velocity of the system from Table 3.

### 3.1 Stars variable in $RV$

Our sample contains four double-lined spectroscopic binaries (SB2): HIP 94924, HIP 95115, HIP 95575, and HIP 97321. Three of them, namely, HIP 94924, HIP 95115, and HIP 97321, have been discovered in this paper; HIP 95575 was discovered to be SB2 by Tokovinin (1991) who also provides the orbital solution for this system. That star has been

then observed with speckle interferometry by Mason et al. (1999) but not resolved.

For one of the new SB2 stars, HIP 97321, we acquired 44 spectrograms that allowed us to compute the orbital solution given in Table 3. In Fig. 1, we plot the  $RV$  light curve of the primary and the secondary component of this system. As can be seen in this figure, typical uncertainties of the  $RV$

measurements of the primary and the secondary component of HIP 97321 are  $\pm 1$  and  $\pm 2$   $\text{km s}^{-1}$ , respectively.

For the three other SB2 systems, HIP 94924, HIP 95115, and HIP 95575, we acquired only few spectrograms. Therefore, more data are needed to compute the orbital solutions of these stars.

For HIP 94112 ( $\langle RV \rangle = -19.72 \pm 0.15$   $\text{km s}^{-1}$ ) and HIP 96062 ( $\langle RV \rangle = -57.74 \pm 0.19$   $\text{km s}^{-1}$ ) the radial velocities measured by us differ by more than  $3\sigma$  from the values reported in the literature which amount to  $-28$   $\text{km s}^{-1}$  for HIP 94112 (Moore & Paddock 1950) and  $-46.6$   $\text{km s}^{-1}$  for HIP 96062 (Fouts & Sandage 1986). However, our determinations agree with  $-18.9 \pm 0.3$   $\text{km s}^{-1}$  and  $-57.8 \pm 0.2$   $\text{km s}^{-1}$  given for these two stars by Nordström et al. (2004) and Latham et al. (2002), respectively. We classify HIP 94112 and HIP 96062 as suspected single-lined spectroscopic binaries.

Finally, we acquired 28 spectrograms spanning 3606 days of the speckle binary HIP 93108 which is a close north-south pair with nominal separation  $1''.7$ . We found that the mean velocities of the components differ by about  $2.6$   $\text{km s}^{-1}$  but we did not detect any obvious acceleration of either star.

We note that none of the double-lined and suspected single-lined binaries discovered in this paper is known to be variable photometrically.

## 4 ATMOSPHERIC PARAMETERS

### 4.1 From Comparison with Standard Stars

For 33 F, G, and K stars observed at OAC, we determined the  $T_{\text{eff}}$ ,  $\log g$  and  $[\text{Fe}/\text{H}]$  using the ROTFIT code (see Frasca et al. 2003, 2006) as described in detail by Molenda-Żakowicz et al. (2007). The method, which has been originally developed by Katz et al. (1998) and Soubiran et al. (1998), consists in comparing the spectra of program stars with a library of spectra of reference stars. The atmospheric parameters of the program stars are computed as the weighted means of the astrophysical parameters of the reference stars which best reproduce the target spectrum. For measuring the similarity of spectra, the value of  $\chi^2$  is used. Then, the weighted standard error ( $\sigma$ ) is computed per each order and the means of each order are averaged using  $(\sigma^{-2} \chi^{-2} f)$  as a weight. Here, the factor  $\chi^{-2}$  accounts for differences between orders due to different S/N and the goodness of the fit, and the factor  $f$  is proportional to the total absorption of lines in each individual order. The  $f$  factor approximately corrects for the different amount of information contained in the blue orders and the red orders with few lines and much continuum, and gives also more weight to orders containing strong and broad lines. As discussed, e.g., by Frasca et al. (2006), this method allows a fast determination of  $T_{\text{eff}}$ ,  $\log g$ , and  $[\text{Fe}/\text{H}]$  of stars of the spectral type F, G, and K, and it can be successfully applied even to spectrograms of low signal-to-noise ratio and moderate resolution.

We used two separate sets of reference spectra to perform independent determinations of  $T_{\text{eff}}$ ,  $\log g$ , and  $[\text{Fe}/\text{H}]$  of our targets. The first set consisted of ELODIE archive spectra (Prugniel & Soubiran 2001) of 246 slowly-rotating stars, the second, of 122 slowly rotating stars ob-

**Table 4.** The astrophysical parameters of 13 new reference stars observed at OAC.

HD	$T_{\text{eff}}$ (K)	$\log g$ (dex)	$[\text{Fe}/\text{H}]$ (dex)	ref.
84441	5310	2.04	-0.28	1
157881	4180	4.70	-0.20	2
169931	3215	0.50	0.00	3
186427	5760	4.40	0.06	2
190007	4650	4.26	0.15	4
191026	5150	3.49	-0.10	2
196755	5510	3.60	-0.09	2
198149	4950	3.41	-0.32	2
201091	4500	4.56	-0.43	2
201092	4120	4.40	-0.63	2
204613	5650	3.80	-0.35	2
212943	4582	2.75	-0.30	2
222404	4810	3.00	0.04	2

[1] McWilliam (1990), [2] Cayrel de Strobel et al. (2001), [3] Prugniel et al. (2007), [4] Soubiran et al. (2008)

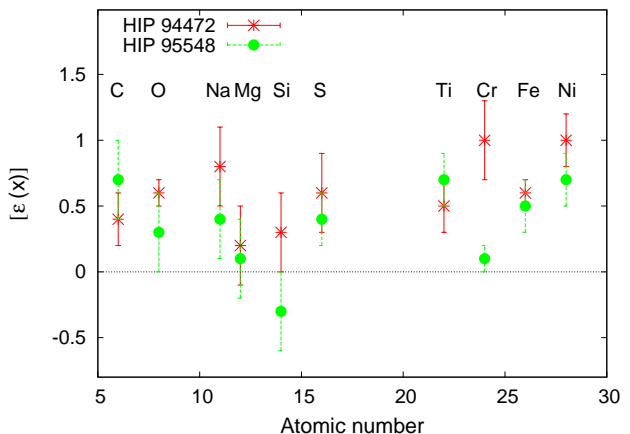


**Figure 3.** The abundance patterns derived for HIP 94472 and HIP 95548 reported in Table 6. For the sake of clarity we excluded from the plot all the chemical elements with  $Z > 28$  (i.e. nickel).

served at OAC with FRESCO. The atmospheric parameters of the 246 stars from the ELODIE archive and of 109 stars from the FRESCO archive have been given by Molenda-Żakowicz et al. (2008). The adopted atmospheric parameters of 13 new reference stars observed with FRESCO in 2009 are given in Table 4, the last column of which contains the references to the bottom of the table where we give the sources of the adopted values of  $T_{\text{eff}}$ ,  $\log g$ , and  $[\text{Fe}/\text{H}]$ .

For computing the atmospheric parameters of stars for which we have multiple exposures, we used the spectrograms of the highest signal-to noise ratio. The values of  $T_{\text{eff}}$ ,  $\log g$ ,  $[\text{Fe}/\text{H}]$ , and their uncertainties derived by means of the ROTFIT method are given in Table 5.

In the sixth column of Table 2, we list also the MK types of the program stars which we inferred by adopting the spectral type and the luminosity class of the reference stars which occurred most frequently. For stars for which we did not perform the spectral classification, we give the spectral classification from the literature.



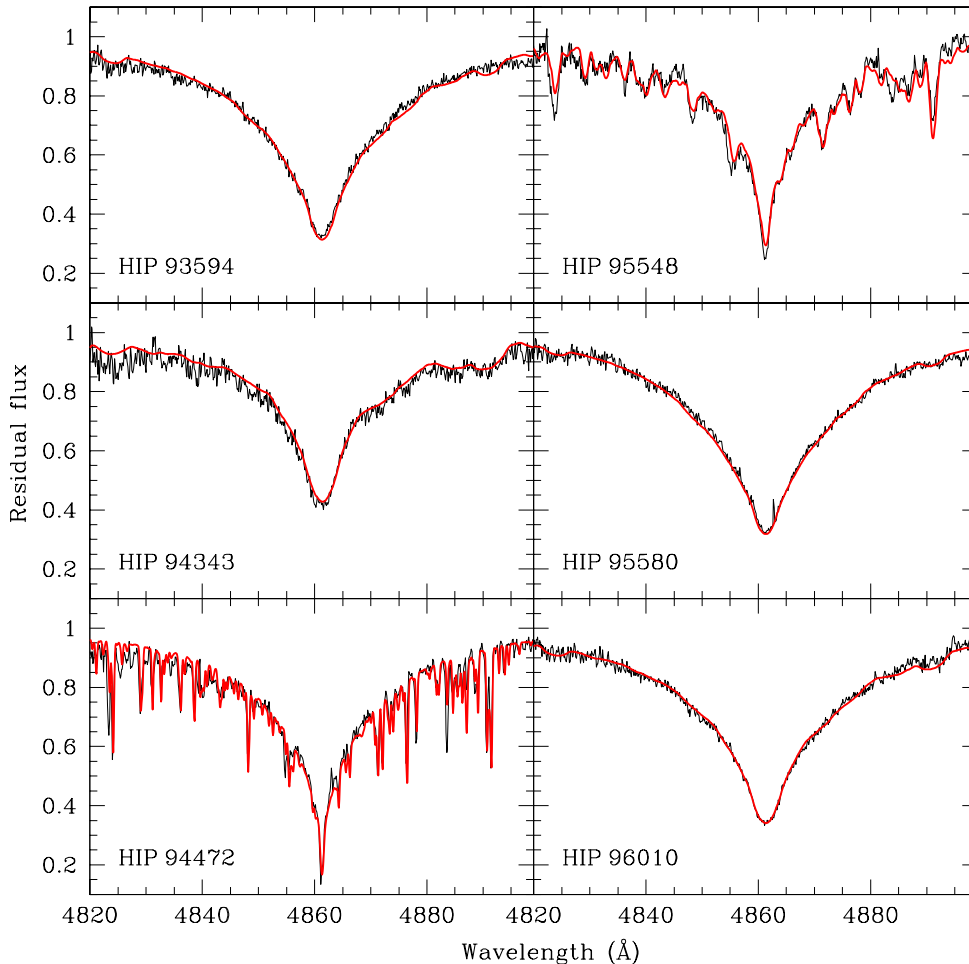


**Figure 2.** The results of fitting of the  $H\beta$  line for the early-type stars observed at OAC.

## 4.2 From Model Atmospheres

### 4.2.1 Stars observed at OAC

The atmospheric parameters of the hot stars observed at OAC, i.e., HIP 94343, HIP 93594, HIP 94472, HIP 95548, HIP 95580, and HIP 96010, were determined by minimizing the difference between the observed and the synthetic  $H\beta$  profiles, using the  $\chi^2$  defined as

$$\chi^2 = \frac{1}{N} \sum \left( \frac{I_{\text{obs}} - I_{\text{th}}}{\delta I_{\text{obs}}} \right)^2 \quad (1)$$

for the measure of the goodness-of-fit parameter, as described in Catanzaro et al. (2010). For starting estimations of  $T_{\text{eff}}$  and  $\log g$ , we used the values from the Kepler Input Catalog.

In Fig. 2, we show the results of fitting the synthetic  $H\beta$  line, computed with SYNTHE (Kurucz & Avrett 1981) on the basis of ATLAS9 (Kurucz 1993) atmosphere models, to the observed  $H\beta$  in the six stars. All the models have been evaluated for solar Opacity Distribution Function and microturbulent velocity  $\xi = 2 \text{ km s}^{-1}$ .

For the slowly rotating stars HIP 94472 and HIP 95548, we determined the photospheric abundances by computing synthetic spectra that reproduce the observed ones. We therefore, divided the measured spectrograms into several intervals, each 25 Å wide, and derived the abundances in each interval by performing a  $\chi^2$  minimization of the difference between the observed and synthetic spectrum. We adopted lists of spectral lines and atomic parameters from Castelli & Hubrig (2004), who updated the parameters listed originally by Kurucz & Bell (1995).

We computed the abundances relative to the solar standard values given by Asplund et al. (2005). For each element, we calculated the uncertainty in the abundance to be the standard deviation of the mean obtained from individual determinations in each interval of the analyzed spectrum. For the elements whose lines occurred in one or two intervals only, the error in the abundance was evaluated by varying the effective temperature and gravity within their uncertainties,  $[T_{\text{eff}} \pm \delta T_{\text{eff}}]$  and  $[\log g \pm \delta \log g]$ , and computing the abundance for  $T_{\text{eff}}$  and  $\log g$  values in these ranges.

For the other four fast rotators, the lines are too broad to attempt this kind of analysis and we derived

only the iron and magnesium abundances from the equivalent widths of Fe I  $\lambda\lambda 5018.44$ ,  $5316.615 \text{ \AA}$  and from Mg II  $\lambda 4481 \text{ \AA}$ . The latter were converted into abundances using WIDTH9 (Kurucz & Avrett 1981) and the ATLAS9 atmospheric models.

In Table 6, we list the derived values of  $T_{\text{eff}}$ ,  $\log g$ ,  $v \sin i$ , the abundances, and the uncertainties of these quantities.

#### 4.2.2 Stars observed with the CfA Digital Speedometers

The atmospheric parameters of stars observed with the CfA Digital Speedometers were derived using synthetic spectra computed by Jon Morse (see Sect. 3) and one-dimensional correlations to identify the template that gives the best match with the observed spectrum. The 7650 template spectra that we used covered a range of  $[4000, 7500]$  in  $T_{\text{eff}}$ ,  $[0, 70]$  in  $v \sin i$ ,  $[2.5, 5.0]$  in  $\log g$ , and  $[-1.5, 0.5]$  in  $[\text{Fe}/\text{H}]$ . The template that we chose gave the highest peak correlation value averaged over all the observed spectra for each program star.

For many of the stars observed with the CfA Digital Speedometers we acquired only a single spectrogram, and some of these exposures are not long enough to reliably extract information about the metallicity because of degeneracy between  $T_{\text{eff}}$ ,  $[\text{Fe}/\text{H}]$ , and  $\log g$  in the spectrum. For this reason, we treated stars with a weak exposure (fewer than 100 counted photons per pixel, corresponding to a signal-to-noise ratio of about 20 per spectral resolution element) differently than stars with a long enough exposure or multiple exposures. For stars with only one weak exposure, we fixed the metallicity to the grid value closest to that determined by ELODIE and FRESCO (or in the literature if that data was not available), and used a cubic spline to interpolate to the peak values in  $\log g$ ,  $T_{\text{eff}}$ , and  $v \sin i$ . For stars with long enough or multiple exposures, we additionally interpolated to the peak  $[\text{Fe}/\text{H}]$  value. The values coming out from our analysis are given in Table 7.

Since the limited number of our observations does not allow us to evaluate statistically significant errors, we adopt the grid spacing, i.e.,  $125 \text{ K}$  in  $T_{\text{eff}}$ ,  $2 \text{ km s}^{-1}$  in  $v \sin i$ , and  $0.25 \text{ dex}$  in  $\log g$  and  $[\text{Fe}/\text{H}]$  as the error estimate.

In Fig. 4, we show the differences between  $T_{\text{eff}}$ ,  $[\text{Fe}/\text{H}]$ , and  $\log g$  derived from the model atmospheres for stars observed with the CfA Digital Speedometers, and the respective parameters computed with the ROTFIT code when using the FRESCO or the ELODIE reference stars. In most cases the values of  $T_{\text{eff}}$ ,  $[\text{Fe}/\text{H}]$ , and  $\log g$  agree to within  $1\sigma$  error bars. We note, though, that the agreement is better for the FRESCO reference stars. This is not surprising, because this grid is composed of reference spectra taken with the same instrument as the target ones.

We put the program stars on the Hertzsprung-Russell (HR) diagram in Fig. 5, using different symbols for stars of  $\log g \leq 3.0$ ,  $3.0 < \log g \leq 4.0$ , and  $\log g > 4.0$ , and using the Hipparcos parallaxes revised by van Leeuwen (2007), and  $T_{\text{eff}}$  from Tables 5, 6 or 7 in this paper. The evolutionary tracks for the solar metallicity as well as the location of the ZAMS for  $Z = 0.019$  (the solar metallicity) and  $Z = 0.001$  are adopted from Girardi et al. (2000). As can be seen in this figure, the location of the program stars in the HR diagram is consistent with the values of  $\log g$  derived in this paper.

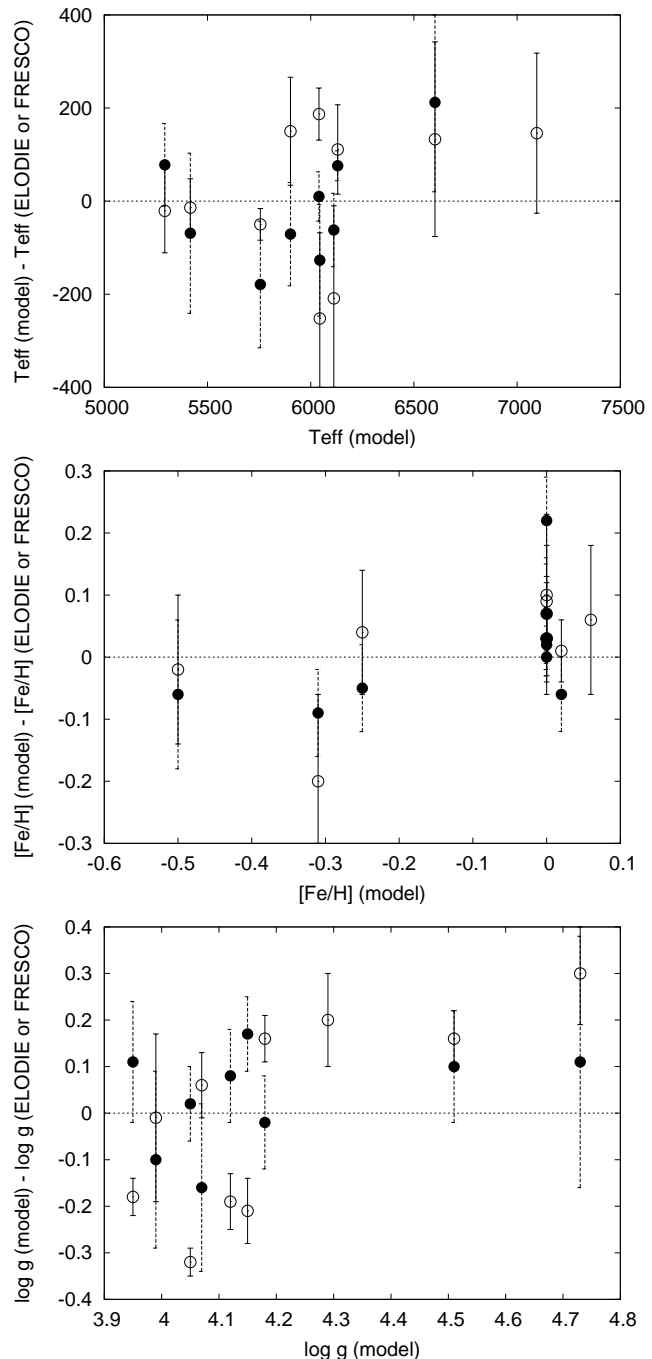


**Figure 4.** The differences between  $T_{\text{eff}}$  (top panel),  $[\text{Fe}/\text{H}]$  (middle panel), and  $\log g$  (bottom panel) derived from the model atmospheres (stars observed with the CfA Digital Speedometers) and with the ROTFIT code (stars observed at OAC.) Filled circles: results obtained with the FRESCO reference stars, open circles: results obtained with the ELODIE reference stars. The zero line is indicated with the dotted lines.

## 5 PROJECTED ROTATIONAL VELOCITY

To derive  $v \sin i$  of the F, G, and K type stars stars observed at OAC, we used the Full Width at Half Maximum (FWHM) method. We applied this method to those orders of the echelle spectra which did not contain broad spectral lines affecting the shape of the cross-correlation function to



**Table 7.** The atmospheric parameters derived from the model atmospheres and the projected rotational velocity,  $v \sin i$ , for the program stars observed with the CfA Digital Speedometers.

HIP	$T_{\text{eff}}$ (K)	$\log g$ (dex)	[Fe/H] (dex)	$v \sin i$ ( $\text{km s}^{-1}$ )
93108A	5916	4.48	-0.27	0.6
93108B	5888	4.55	-0.23	2.0
93556	6112	4.07	-0.31	52.6
93657	5756	4.15	0.02	4.6
94071	6602	4.18	0.00	17.4
94798	7095	4.29	0.06	36.8
94922	6040	4.12	0.00	10.3
94931	4963	4.36	-0.53	1.1
95274	5417	4.05	0.00	5.0
95568	5760	3.59	0.00	5.6
95575 <sup>a</sup>	4734	4.21	-0.37	13.5
95876	6044	3.99	-0.50	11.2
96062	6266	4.04	0.00	63.5
96561	5293	4.73	0.00	3.0
97236	6131	3.95	0.00	9.1
97321 A <sup>b</sup>	6350	4.50	0.00	6.0
97321 B <sup>b</sup>	5500	4.50	0.00	2.0
97706	5730	3.75	0.00	15.2

<sup>a</sup> The atmospheric parameters and the  $v \sin i$  are derived from the composite spectrum.

<sup>b</sup> The stellar parameters are those that maximize the weighted mean correlation coefficient in the TODCOR solution that uses fixed  $\log g = 4.5$  and  $[m/H]=0$ .

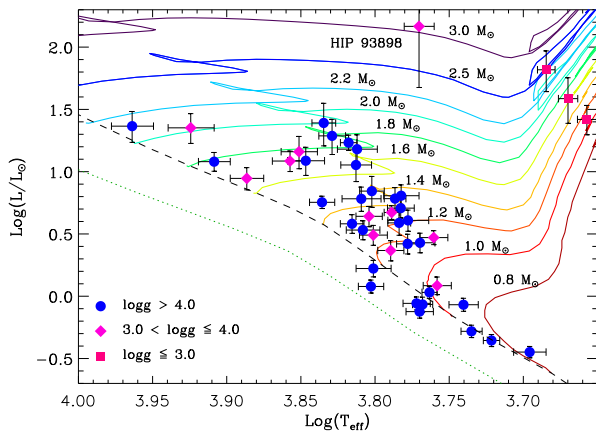


**Figure 5.** The HR diagram for stars discussed in this paper. Different symbols are used to indicate stars of different  $\log g$ . The evolutionary tracks from Girardi et al. (2000) are plotted with solid lines; the ZAMS for  $Z = 0.019$  and  $Z = 0.001$  is plotted, respectively, with the dashed and dotted lines.

compute the mean projected rotational velocities. As templates, we used a grid of artificially broadened spectra of non-rotating stars that have  $T_{\text{eff}}$ ,  $\log g$ , and  $[\text{Fe}/\text{H}]$  similar to the parameters of the program stars.

For the hot stars observed at OAC and the stars observed with the CfA Digital Speedometers, we deter-

mined  $v \sin i$  simultaneously with the atmospheric parameters when computing the best fit of the synthetic spectrum to the observed one. An upper limit of 5 and 2  $\text{km s}^{-1}$  in  $v \sin i$  has been estimated according to the instrumental resolution of the spectrographs, as discussed in Molenda-Żakowicz et al. (2007).

We find that one of the early-type stars, HIP 94472, is rotating slowly ( $v \sin i = 13 \text{ km s}^{-1}$ ) which makes it a promising target for asteroseismic modeling. The star might still be a fast rotator seen pole-on, but we remark that Bidelman classifies this star to the spectral type Am. We also found the abundance pattern typical of Am stars that are slow rotators. Thus, we conclude that HIP 94472 is very likely a slowly rotating star.

The derived values of  $v \sin i$  of our program stars are given in the last columns of Tables 5, 6, and 7

## 6 DISCUSSION

### 6.1 The effective temperature

We compared the atmospheric parameters of the program stars derived in this paper with the determinations from the literature. For 11 stars from this paper, the effective temperature was derived from photometric indices by Nordström et al. (2004), Masana et al. (2006), Alonso et al. (1996), González Hernández & Bonifacio (2009), Casagrande et al. (2006), Fulbright & Johnson (2003), Gray et al. (2003), and Allende Prieto & Lambert (1999) (who derive  $T_{\text{eff}}$  from the comparison of the stars' position in the colour-magnitude diagram with the evolutionary models of solar metallicity); spectroscopic determinations by Robinson et al. (2007), Soubiran et al. (2008), and Tomkin & Lambert (1999) are available for seven stars. For most of the stars,  $T_{\text{eff}}$  in this paper and the values from the literature agree satisfactorily. Only for HIP 97071,  $T_{\text{eff}}$  derived by Nordström et al. (2004) and Masana et al. (2006) from  $uvby\beta$  and  $JHK$  photometry is around 300 K higher. Such a discrepancy, though, is not unusual taking into account that even a moderate error in the adopted  $E(B - V)$  can imply an error of 100 K or more in the photometric effective temperature (see, e.g., Casagrande et al. 2010).

The comparison of  $T_{\text{eff}}$  in this paper with the values given in the Kepler Input Catalog (KIC) for 30 stars from our sample shows that in most cases the discrepancies do not exceed  $\pm 200$  K – see Fig. 6 where we plot the differences between the atmospheric parameters derived in this paper and the values listed in the KIC. The highest discrepancies occur for HIP 93898 and HIP 96010 for which the KIC lists  $T_{\text{eff}}$  lower by around 1300 K. For the former star, also  $\log g$  and  $[\text{Fe}/\text{H}]$  in this paper are significantly different from the values provided in the KIC.

The reason for so large discrepancies in the atmospheric parameters of HIP 93898 may be the fact that this is a close binary separated by  $0''.5$ . The difference of brightness between the components is 2.5 mag. Given the proximity of the stars, HIP 93898 is very likely a physical binary. Thus, the secondary component may be significantly cooler and redder than the primary. This could affect the broad-band photometry spanning a wide wavelength range, like that used for

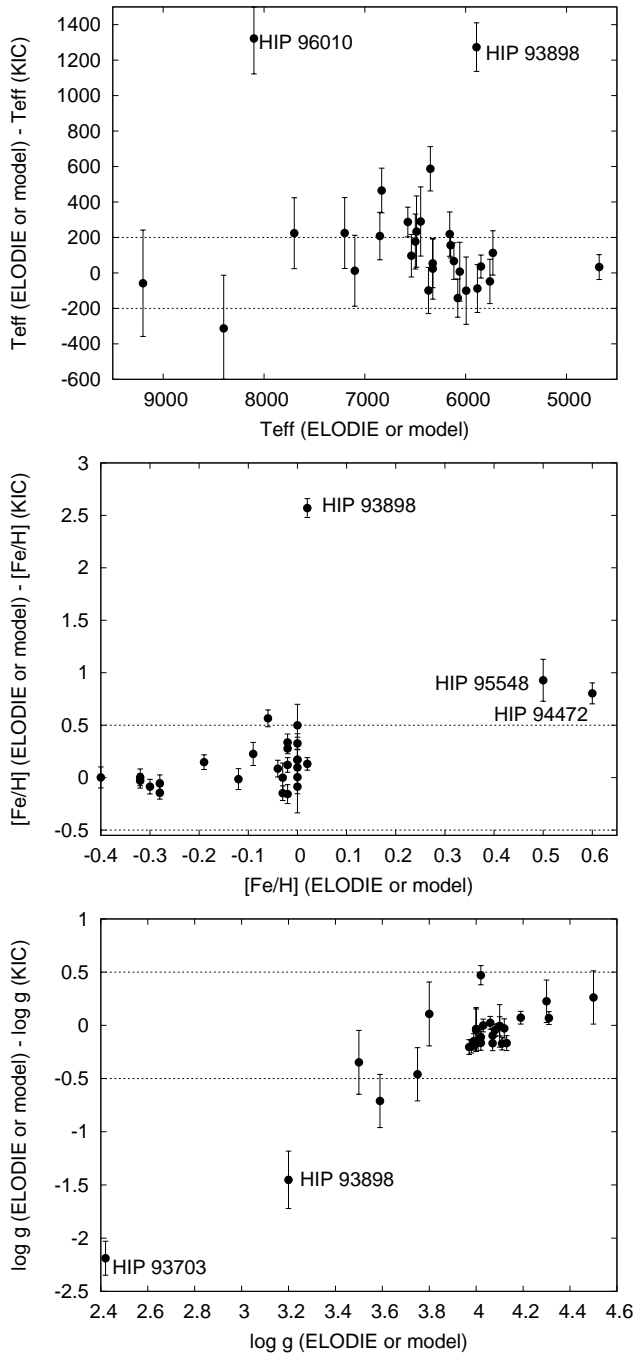


**Figure 6.** The differences between  $T_{\text{eff}}$  (*top panel*),  $[\text{Fe}/\text{H}]$  (*middle panel*), and  $\log g$  (*bottom panel*) derived in this paper with the use of the reference stars from the ELODIE library (F, G, and K stars) or from the model atmospheres (hot stars) and the values of  $T_{\text{eff}}$ ,  $[\text{Fe}/\text{H}]$  and  $\log g$  in the Kepler Input Catalog. The dotted lines represent the stated uncertainty of the atmospheric parameters in the KIC.

deriving the atmospheric parameters in the KIC but the contamination of the optical spectrum should be marginal and its influence on the atmospheric parameters derived in this paper, negligible. This conclusion is supported by the fact that  $T_{\text{eff}}$  derived by us using the grid of Moon & Dworetzky (1985) and the narrow-band Strömgren indices provided by

Hauck & Mermilliod (1990), 5797 K, agrees well with the spectroscopic value.

We note also that HIP 93898 falls in a very particular position in the HR diagram (see Fig. 5) at which the evolution is very fast. Since this region of the HR diagram is sparsely populated, stars discovered to fall in that location are very interesting objects which deserve further study.

The reason why our value of  $T_{\text{eff}}$  derived for HIP 96010 is significantly higher than in the KIC is not clear, and the literature does not provide photometric measurements which could be used to confirm the effective temperature derived in this paper. We note, though, that also this star is listed as an astrometric binary by Makarov & Kaplan (2005).

## 6.2 The metallicity

For 16 stars from our sample, the metallicity was derived either from photometry by Nordström et al. (2004), Ibukiyama & Arimoto (2002), Alonso et al. (1996), Zakhohaj & Shaparenko (1996), and Gray et al. (2003) or from spectroscopy by Robinson et al. (2007), Soubiran et al. (2008), Fulbright & Johnson (2003), Tomkin & Lambert (1999), Thévenin & Idiart (1999), and Peterson (1981). All these derivations agree with the values derived in this paper to within  $1-2\sigma$  error bars. The highest discrepancy occurs for the subdwarf HIP 94931 for which we derive the mean  $[\text{Fe}/\text{H}] = -0.30$  dex which agrees with  $[\text{Fe}/\text{H}] = -0.29$  derived from photometry by Ibukiyama & Arimoto (2002) but not with the value derived by Peterson (1981) from high-resolution spectroscopy,  $[\text{Fe}/\text{H}] = -0.74 \pm 0.13$ .

The comparison of  $[\text{Fe}/\text{H}]$  in this paper with those given in the KIC shows that for most stars the differences do not exceed  $\pm 0.5$  dex, which is the stated uncertainty of the values in the KIC. The highest discrepancies occur for HIP 93898 (2.6 dex) which was discussed in the previous section, HIP 95548 (1 dex), and HIP 94472 (0.8 dex), classified by Bidelman (1985) to the spectral type Am, which indeed shows an enhanced pattern of metals in its photosphere in our analysis. We do not find any indications of duplicity of that last star suggested by the spectral type F+A: assigned by Skiff (2010), either from the radial velocity or from the spectrum appearance.

## 6.3 The surface gravity

The surface gravity was derived spectroscopically for ten of our program stars by Robinson et al. (2007), Soubiran et al. (2008), Tomkin & Lambert (1999), and Thévenin & Idiart (1999), or from photometry by Allende Prieto & Lambert (1999), Gray et al. (2003), and Fulbright & Johnson (2003). For all these stars, the  $\log g$  values agree with our determinations to within  $1-2\sigma$  error bars.

The differences in  $\log g$  derived in this paper and those listed in the KIC do not exceed 0.2 dex for most stars, and for all but one fall into the range of the stated precision of  $\log g$  in the KIC to within their  $1\sigma$  error bars. The highest discrepancies occur for the already discussed star HIP 93898, and for HIP 93703 which turns out to be a giant, unlike the KIC determination.

## 7 SUMMARY

We derived the atmospheric parameters, the radial velocity, and the projected rotational velocity of 44 stars selected as *Kepler* asteroseismic targets from the stars proposed by A.F. and J.M-Ž. in the first run of the *Kepler* proposals; to 33 of these stars we assigned the MK types.

We discovered three double-lined spectroscopic binary systems, HIP 94924, HIP 95115, and HIP 97321, and we classify two other stars, HIP 94112 and HIP 96062, as suspected single-lined spectroscopic binaries. For one of the SB2 stars discovered in this paper, HIP 97321, we provide the orbital solution. The other SB2 systems require more observations to derive their orbital periods and compute the orbital elements.

The values of the projected rotational velocity which we provide can be used as a guideline for making selection of long-term asteroseismic targets for the *Kepler* space mission. Our measurements can, e.g., help reject very fast rotators for which an asteroseismic modeling is difficult.

The precision of the atmospheric parameters given in this paper will allow to derive the mean density of the stars and to compute the mass and radius of the stars with a precision better than 3% when these parameters are combined with the large separation of the frequencies detected in the *Kepler* magnitudes. The derived radii may be then used to constrain accurate dimensions of transiting planets (Christensen-Dalsgaard et al. 1997) and to refine the scientific output of the *Kepler* mission (Borucki et al. 2009). Since the stellar mean densities can be also derived from the analysis of the light curve of the transiting planets, a comparison of the densities derived in these two completely independent ways will give a direct test of the physics involved. Then, our measurements allowed us to complete the information on the atmospheric parameters which is missing in the KIC for 14 stars from our sample, and to verify the values of  $T_{\text{eff}}$ , [Fe/H], and  $\log g$  listed in the KIC for the remaining 30 stars.

We found that although for most of the discussed stars  $T_{\text{eff}}$ ,  $\log g$  and [Fe/H] in this paper and in the KIC agree to within the KIC uncertainties, for some the differences can be high. The stars for which we report the highest discrepancies between  $T_{\text{eff}}$ , [Fe/H], and  $\log g$  in this paper and in the KIC are HIP 93703, HIP 93898, HIP 94472, HIP 95548, and HIP 96010.

Our results show that ground-based studies aiming at deriving atmospheric parameters of *Kepler* asteroseismic targets are crucial for the successful asteroseismic modeling of these stars, and for making a full use of the potential of the *Kepler* space mission.

## ACKNOWLEDGMENTS

This work has been partly supported by *Kepler* mission under cooperation agreement NCC2-1390 (D.W.L., PI), the Italian *Ministero dell'Istruzione, Università e Ricerca* (MIUR), and the Polish MNiSW grant N203 014 31/2650 which are gratefully acknowledged.

## REFERENCES

- Baird S.R., 1981, ApJ, 245, 208  
 Allende Prieto, C., & Lambert, D. L. 1999, A&A, 352, 555  
 Alonso, A., Arribas, S., & Martinez-Roger, C. 1996, A&AS, 117, 227  
 Asplund, M., Grevesse, N., & Sauval, A. J. 2005, in *Cosmic Abundances as Records of Stellar Evolution and Nucleosynthesis*, eds. T. G. Barnes III & F. N. Bash, ASP Conf. Ser., 336, 25  
 Bidelman, W. P. 1985, AJ, 90, 341  
 Borucki, W., Koch, D., Batalha N., et al. 2009, “Transiting Planets”, Proc. of the IAU Symp., 253, 289  
 Casagrande, L., Portinari, L., & Flynn, Ch. 2006, MNRAS, 373, 13  
 Casagrande, L., Ramírez, I., Meléndez, J., Bessell, M., & Asplund, M. 2010, A&A, 512, A54  
 Catanzaro, G., Frasca, A., Molenda-Żakowicz, J., & Marilli, E. 2010, A&A preprint doi <http://dx.doi.org/10.1051/0004-6361/201014189>  
 Castelli, F., & Hubrig, S. 2004, A&A, 425, 263  
 Cayrel de Strobel, G., Soubiran, C., & Ralite N. 2001 A&A, 373, 159  
 Chaplin, W. J., Appourchaux, T., Elsworth, Y., et al. 2010, ApJ, 713L, 169  
 Christensen-Dalsgaard, J., Arentoft, T., Brown, T. M., et al. 2007, Comm. in Aster., 150, 350  
 Christensen-Dalsgaard, J., Kjeldsen, H., Brown, T. M., et al. 2010, ApJ, 713L, 164  
 ESA 1997, The Hipparcos Catalogue, ESA SP-1200  
 Evans, D. S. 1967, IAU Symp. 30, Eds. A. H. Batten and J. F. Heard, Academic Press, London, p.57  
 Fekel, F. C. 1999, in *Precise Stellar Radial Velocities*, eds. J. B. Hearnshaw & C. D. Scarfe, ASP Conf. Ser., 185, 378  
 Fouts, G., & Sandage A. 1986 AJ, 91, 1189  
 Frasca, A., Alcalà, J. M., Covino, E., et al. 2003, A&A, 405, 149  
 Frasca, A., Guillout, P., Marilli, E., et al. 2006, A&A, 454, 301  
 Fulbright, J. P., & Johnson, J. A. 2003, ApJ, 595, 1154  
 Gilliland, R. L. Brown, T. M. Christensen-Dalsgaard, J., et al. 2010, PASP, 122, 131  
 Girardi, L., Bressan, A., Bertelli, G., & Chiosi, C. 2000, A&A, 141, 371  
 González Hernández, J. I., & Bonifacio, P. 2009, A&A, 497, 497  
 Gray, R. O., Corbally, C. J., Garrison, R. F., McFadden, M. T., & Robinson, P. E. 2003, AJ, 126, 2048  
 Grenier, S., Baylac, M. O., Rolland, L., et al. 1999, A&AS, 137, 451  
 Hauck, B., & Mermilliod, M. 1990, A&AS, 86, 107  
 Ibukiyama, A., & Arimoto, N. 2002, A&A, 394, 927  
 Katz, D., Soubiran, C., Cayrel, R., Adda, M., & Cautain, R. 1998, A&A, 338, 151  
 Kurucz, R. L. 1993, in *Peculiar versus Normal Phenomena in A-type and Related Stars*, eds. M. M. Dworetzky, F. Castelli, & R. Faraggiana, ASP Conf. Ser., 44, p.87  
 Kurucz, R. L., & Avrett, E. H. 1981, SAO Special Rep., 391  
 Kurucz, R. L., & Bell B. 1995, Kurucz CD-ROM No. 23. Cambridge, Mass.: Smithsonian Astrophysical Observatory

- Latham, D. W., Brown, T. M., Monet, D. G., et al. 2005, *Bull. Amer. Astron. Soc.*, 37, 1340
- Latham, D. W., Mazeh, T., Stefanik, R. P., et al. 1992, *AJ*, 104, 774
- Latham, D. W., Stefanik, R. P., Torres, G., et al. 2002, *AJ*, 124, 1144
- van Leeuwen F. 2007, *A&A*, 474, 653
- Makarov, V. V., & Kaplan, G. H. 2005, *AJ*, 129, 2420
- Masana, E., Jordi, C., & Ribas, I. 2006, *A&A*, 450, 735
- Mason, B. D., Martin, C., Hartkopf, W. I., et al. 1999, *AJ*, 117, 1890
- McWilliam, A. 1990 *ApJ Supp. Ser.*, 74, 1075
- Molenda-Żakowicz, J., Bruntt, H., Sousa, S., et al. 2010, arXiv: 1005.0986
- Molenda-Żakowicz, J., Frasca, A., & Latham, D.W. 2008, *Acta Astron.*, 58, 419
- Molenda-Żakowicz, J., Frasca, A., Latham D.W., & Jerzykiewicz M. 2007, *Acta Astron.*, 57, 301
- Moon, T. T., & Dworetzky, M. M. 1985, *MNRAS*, 217, 305
- Moore, J. H., & Paddock, G. F. 1950, *ApJ*, 112, 48
- Nordström, B., Mayor, M., Andersen, J., et al. 2004, *A&A*, 418, 989
- Peterson, R.C. 1981, *ApJ*, 244, 989
- Prugniel, Ph., & Soubiran, C. 2001, *A&A*, 369, 1048
- Prugniel, P., Soubiran, C, Koleva, M., & Le Borgne, D. 2007, ELODIE library V3.1, astro-ph/0703658
- Robinson, S. E., Ammons, S.M., Kretke K.A., et al. 2007, *ApJ Supp. Ser.*, 169, 430
- Royal Observatory, Greenwich, 1935, *Second Greenwich Catalog of Stars for 1925.0 (London 1935)*
- Sato, K., & Kuji, S. 1990, *A&AS*, 85, 1069
- Skiff, B. A. 2010, *General Catalogue of Stellar Spectral Classifications*, Lowell Observatory
- Soubiran, C., Bienayme, O., Mishenina, T. V., & Kovtyukh, V. V. 2008, *A&A*, 480, 91
- Soubiran, C., Katz, D., & Cayrel, R. 1998, *A&AS*, 133, 221
- Sozzetti, A., Torres, G., Chrbonneau, D., et al. 2007, *ApJ*, 664, 1190
- Stefanik, R.P., Latham, D.W., & Torres, G. 1999, *Precise Stellar Radial Velocities*, ASP Conf. Ser. 185, IAU Coll. 170, Eds. J. B. Hearnshaw and C. D. Scarfe, p. 354
- Stello, D., Chaplin, W. J., Bruntt, H. et al. 2009, *ApJ*, 700, 1589
- Thévenin, F., & Idiart, T. P. 1999, *ApJ*, 521, 753
- Thompson G.I., Nandy K. Jamar C., Monfils A. Houziaux L., Carnochan D.J., Wilson R. 1978, *Catalogue of Ultraviolet Stellar Fluxes (TD1)*
- Tokovinin, A. A. 1991, *A&AS*, 91, 497
- Tomkin, J., & Lambert, D. L. 1999, *ApJ*, 523, 234
- Tonry, J., & Davis, M. 1979, *AJ*, 84, 1511
- Topping, J. 1972, *Errors of Observation and Their Treatment*, Chapman and Hall Ltd., 92
- Torres, G., Boden, A. F., Latham, D.W., Pan, W., & Stefanik, R. 2002, *AJ*, 124, 1716
- Udry, S., Mayor, M., Maurice, E., et al. 1999, in *Precise Stellar Radial Velocities ASP Conf. Ser.*, 185, 383
- Uytterhoeven, K., Szabo, R., Southworth, J. et al. 2010, arXiv:1003.6089
- Wilson O. C. 1962, *ApJ*, 136, 793
- Wright, C. O., Egan, M. P., Kraemer, K. E., & Price, S. D. 2003, *AJ*, 125, 359
- Zakhochaj, V. A., & Shaparenko, E. F. 1996, *Kinematika Fiz. Nebesn. Tel.*, 12, no 2, p. 20
- Zucker, S., & Mazeh, T. 1994, *ApJ*, 420, 806